Published in final edited form as:
Proteomics. 2009 March ; 9(5): 1241–1253. doi:10.1002/pmic.200800636.

Proteome of synaptosome-associated proteins in spinal cord dorsal horn after peripheral nerve injury

Om V. Singh[1,*], **Myron Yaster**[2], **Ji-Tian Xu**[2], **Yun Guan**[2], **Xiaowei Guan**[2], **Arun M. Dharmarajan**[3], **Srinivasa N. Raja**[2], **Pamela L. Zeitlin**[1], and **Yuan-Xiang Tao**[2]

[1]Department of Pediatrics, Johns Hopkins University School of Medicine, Baltimore, Maryland 21205, USA

[2]Department of Anesthesiology and Critical Care Medicine, Johns Hopkins University School of Medicine, Baltimore, Maryland 21205, USA

[3]School of Anatomy & Human Biology, The University of Western Australia, Crawley, Perth Western 6009, Australia

Abstract

Peripheral nerve injury may lead to neuroadaptive changes of cellular signals in spinal cord that are thought to contribute to central mechanisms underlying neuropathic pain. Here we used a two-dimensional electrophoresis (2-DE)-based proteomic technique to determine the global expression changes of synaptosome-associated proteins in spinal cord dorsal horn after unilateral fifth spinal nerve injury (SNI). The fifth lumbar dorsal horns ipsilateral to SNI or sham surgery were harvested on day 14 post-surgery, and the total soluble and synaptosomal fractions were isolated. The proteins derived from the synaptosomal fraction were resolved by 2-DE. We identified 27 proteins that displayed different expression levels after SNI, including proteins involved in transmission and modulation of noxious information, cellular metabolism, membrane receptor trafficking, oxidative stress, apoptosis, and degeneration. Six of the 27 proteins were chosen randomly and further validated in the synaptosomal fraction by Western blot analysis. Unexpectedly, Western blot analysis showed that only one protein in the total soluble fraction exhibited a significant expression change after SNI. The data indicate that peripheral nerve injury changes not only protein expression but also protein subcellular distribution in dorsal horn cells. These changes might participate in the central mechanism that underlies the maintenance of neuropathic pain.

Keywords

Peripheral nerve injury; Two-dimensional electrophoresis; Spinal cord dorsal horn; Synaptosomal fraction

1 Introduction

Neuropathic pain is a common syndrome that results from disease or dysfunction in the nervous system, such as from peripheral nerve or spinal cord injury [1,2]. It is characterized by spontaneous ongoing or intermittent burning pain, an exaggerated response to painful stimuli, and pain in response to normally innocuous stimuli. Despite considerate research into the neurobiological mechanisms of neuropathic pain during the past decades, our understanding

Corresponding author: Yuan-Xiang Tao, Associate Professor, Department of Anesthesiology and Critical Care Medicine, Johns Hopkins University School of Medicine, 720 Rutland Ave., 355 Ross, Baltimore, MD 21205. Tel: +1-410-614-1848; Fax: +1-410-614-7711.
[*]Current Address: Division of Biological and Health Sciences, University of Pittsburgh, Bradford, PA 16701, USA

of this disorder is still incomplete, and its treatment by current drugs, such as antidepressants, anticonvulsants, opioids, and non-steroidal anti-inflammatory drugs, is often inadequate [1, 2].

Evidence indicates that peripheral nerve injury might lead to neuroadaptive changes of cellular signals in dorsal horn; such changes are thought to contribute to the central mechanisms that underlie neuropathic pain [1,2]. The global changes of gene expression in dorsal horn following peripheral nerve injury recently have been demonstrated by cDNA microarray [3-5]. Some translational protein products have been further confirmed by Western blot and immunohistochemistry [3,4]. For example, peripheral nerve injury increases expression of both mRNA and protein for protein kinase C alpha, protein kinase beta 1, and calcium channel alpha 2/delta subunit 1 [3]. However, these studies confirmed only the expression changes of some selected genes of interest at the protein level. It is possible that peripheral nerve injury could alter the expression of some genes without affecting their protein expression. In addition, peripheral nerve injury might modulate post-transcriptional regulation of some proteins without affecting gene expression. A previous study showed that peripheral inflammation increased protein but not mRNA levels for the transient receptor potential ion channel TRPV1 in the dorsal root ganglion [6]. Accordingly, the global neuroadaptive changes of cellular signaling proteins in dorsal horn under neuropathic pain conditions are still unclear.

Proteomic analysis can provide expression profiles of proteins and their post-translational modifications in cells, tissues, and organs [7,8]. Using proteomic approaches, Lee *et al*. [9] first reported on five proteins that displayed differential expression in spinal cord after spinal nerve injury (SNI). Later, Kunz *et al.* [10] also found five regulated proteins in the spinal cord after chronic constriction injury. Interestingly, according to current knowledge, these identified proteins are involved in oxidative stress, apoptosis, or cellular metabolism, but not in nocicepetive transmission and modulation. In addition, many important classes of proteins that undergo significant expression changes in dorsal horn under neuropathic pain conditions [3, 4], were not identified in those proteomic studies [9,10]. Therefore, more in-depth proteomic analysis is required to study nerve injury-induced global changes in protein expression in the spinal dorsal horn.

In the present study, we first isolated the crude synaptosomal fraction derived from spinal dorsal horn of rats on day 14 after fifth lumbar SNI or sham surgery and then used two-dimensional gel electrophoresis (2-DE) in combination with mass spectrometry to examine the global changes of synaptosome-associated proteins in dorsal horn under neuropathic pain conditions. Finally, we used Western blot analysis to further validate the proteomic analysis by examining the expression changes in six of the proteins identified in the synaptosomal and total soluble fractions.

2 Materials and methods

2.1 Animal preparations

Male Sprague-Dawley rats (250–350 g) were housed individually in cages on a standard 12 h-12 h light-dark cycle. Water and food were available *ad libitum* until rats were transported to the laboratory approximately 1 h before the experiments. All animal experiments were carried out with the approval of the Institutional Animal Care and Use Committee at the Johns Hopkins University and were consistent with the ethical guidelines of the National Institutes of Health and the International Association for the Study of Pain. All efforts were made to minimize the number of animals used and their suffering.

2.2 SNI-induced neuropathic pain model

Experimental animals (n = 9 rats) were anesthetized with isoflurane and placed in a prone position. A dorsolateral skin incision was made on the lower back. The sixth lumbar transverse process was identified and freed of its muscle attachments and then removed. The underlying fifth lumbar nerve root was isolated, ligated with a 3-0 silk suture, and transected just distal to the ligature according to the method described previously [11,12]. After appropriate hemostasis, the muscle layer was closed with a silk suture and the skin stapled. In the sham group (n = 9 rats), the surgical procedure was identical to that described above, except that the fifth lumbar spinal nerve was not ligated and transected.

2.3 Behavioral responses to mechanical stimuli

Behavioral testing was performed by experimenters blinded to the rats' surgical group. Each animal (18 rats, 9/group) was placed in a Plexiglas chamber on an elevated mesh screen. Behavioral acclimation was allowed for at least 30 min. Mechanical paw withdrawal thresholds (PWTs) were measured with the up–down testing paradigm [13,14] 1 day prior to surgery and on day 14 after SNI or sham surgery. von Frey hairs in log increments of force (0.38, 0.57, 1.23, 1.83, 3.66, 5.93, 9.13, 13.1 g) were applied for a duration of 4–6 s to the region between the foot pads in the plantar aspect of the hindpaw. The 1.83-g stimulus was applied first. If a positive response occurred, the next smaller von Frey hair was used; if a negative response was observed, the next higher force was used. The test was continued until: (1) the responses to five stimuli were assessed after the first crossing of the withdrawal threshold or (2) the upper/lower end of the von Frey hair set was reached before a positive/negative response had been obtained. Abrupt paw withdrawal, licking, and shaking were regarded as positive responses.

2.4 Subcellular fractionation of proteins

Biochemical fractionation was carried out according to previous studies with minor modification [15,16]. Briefly, the animals were sacrificed by decapitation after behavioral testing. The fifth lumbar spinal cord segments ipsilateral to SNI (n = 9 rats) or sham surgery (n = 9 rats) were collected. The dorsal part of the spinal cord was separated from the ventral part. Because the L_5 dorsal horns of rats are extremely small, the tissue from 3 rats was pooled together to obtain enough protein to conduct both 2-DE and Western blotting analyses (see below). These two analyses were repeated three times. The tissues were homogenized in homogenization buffer [10 mM Tris-HCl (pH 7.4), 5 mM NaF, 1 mM sodium orthovanadate, 320 mM sucrose, 1 mM EDTA, 1 mM EGTA, 0.1 mM phenylmethylsulfonyl fluoride, 1 M leupeptin, and 2 mM pepstatin A]. After centrifugation at 1,000 × *g* for 20 min at 4°C, the supernatant (S1, total soluble fraction) was collected and the pellet (P1, nuclei and debris fraction) discarded. After measurement of the protein concentration, 20% of the supernatant (S1) was removed to measure the amounts of dorsal horn proteins in the total soluble fraction. The remaining supernatant (S1, 80%) was centrifuged at 10,000 × *g* for 20 min to produce a pellet (P2) and supernatant (S2). The P2 was lysed hypo-osmotically in water and centrifuged at 25,000 × *g* to produce a pellet (P3). The S2 was considered to be the crude cytosolic fraction and the P3 the crude synaptosomal membrane fraction [15,16].

2.5 Two-dimensional gel electrophoresis

Two-dimensional gel electrophoresis (2-DE) was performed as previously described with modifications [17,18]. Briefly, the synaptosomal membrane fraction (P3) was dissolved in 2-DE lysis buffer [8 M urea, 4% CHAPS, and 20 mM Tris-HCl (pH 8.8)]. Total protein (50 μg) was separated by first-dimensional isoelectric focusing (IEF) using pre-cast, dry, 17-cm immobilized pH gradient (IPG) strips (pH 3–10; Bio-Rad, Hercules, CA) on a IPGphore unit (Bio-Rad). In brief, each IPG strip was first hydrated for 12 h with the protein in 300 μL of IEF hydration buffer (7 M urea, 2 M thiourea, 4% CHAPS, 0.5% carrier ampholyte, 40 mM

dithiothreitol, and 0.002% bromophenol blue). IEF was carried out using the following conditions: (1) 250 V for 20 min on linear ramp, (2) 10,000 V for 2 h on linear ramp, (3) 10,000 V at 45,000 V/h on rapid ramp, (4) holding at 500 V on rapid ramp until IPG strips were removed from the first dimension. The strips were then subjected to a two-step equilibration using equilibration buffer I [6 M urea, 2% SDS, 0.375 M Tris-HCl (pH 8.8), 20% glycerol, and 130 mM dithiothreitol] followed by equilibration buffer II [6 M urea, 2% SDS, 0.375 M Tris-HCl (pH 8.8), 20% glycerol, and 135 mM iodoacetamide] for 15 min each just before 2-DE. The second dimensional electrophoresis was performed on 1.0-mm 10% SDS-PAGE gels using an Amersham Pharmacia Iso-DALT electrophoresis unit at 50 V for 30 min followed by 100 W until the blue dye front arrived at the bottom of the gel.

2.6 Image acquisition and 2-DE gel spot pattern analysis

Any two gels undergoing direct comparison were run and silver stained in parallel. Silver staining was performed with the MS-compatible SilverQuest™ Silver staining kit (Invitrogen, Carlsbad, CA). Stained gel images were acquired with Molecular Imager FX (Bio-Rad). Progenesis software version 2005 (Nonlinear Dynamics, Durham, NC) was used in the present study for spot detection, gel alignment, spot quantification, and log normalized data. The data from the SNI-treated groups and corresponding with the silver-stained spots of sham group were generated from three parallel experiments. The analysis of variance (ANOVA) generated from Progenesis software was applied to compare the log normalized data derived from the spots of the SNI-treated groups and the sham groups [17-19]. Based on the gel-to-gel variation of less error in highly abundant proteins, significant protein spots that showed at least 2-fold difference in the spot relative volume between two groups were selected for protein identification.

2.7 Enzymatic digestion of protein spots

Selected silver-stained protein spots were excised manually with a plastic plunger (The gel, San Francisco, CA) and transferred to a microcentrifuge tube pre-rinsed with acetonitrile (500 μL). In addition to these protein spots, 20 blank gel pieces were excised from the gel to use as controls. Prior to peptide digestion, the protein gel pieces were destained with a 1:1 mix of 30 mM potassium ferrocyanide and 100 mM sodium thiosulphate until they lost the brown color and then were washed three times with 200 μL proteomics-grade water (Bio-Rad). Destained gel pieces were washed with 20 mM NH_4HCO_3 and dehydrated with acetonitrile twice for 10 min each. Finally the dried gel pieces were hydrated in 20 μl of sequencing-grade modified trypsin (10 ng/μL, Promega, Madison, WI) in 20 mM NH_4HCO_3 (pH 8.5, Sigma, St. Louis, MO) and incubated on ice for 45 min. Excess trypsin was removed and replaced with 10 mM NH_4HCO_3. Protein digestion was continued by incubating the gel pieces at 37°C overnight with gentle shaking. Peptides were extracted from gel pieces by adding 200 μL of 0.1% trifluoroacetic acid in 60% acetonitrile followed by vigorous shaking for 60 min at 30°C. Supernatant was collected and dried in a speed vacuum concentrator (Eppendorf, Westbury, NY), and the resulting peptides were solubilized in 5 μL of 0.1% trifluoroacetic acid.

2.8 Peptide mass fingerprinting by mass spectrometry

The extracted peptide mixture was desalted with an in-tip reversed phase column (C18 Zip-Tip; Millipore) [17]. The peptide mixture was eluted from the Zip-Tip with 2 μL of matrix solution (10 mg/mL α-cyano-4-hydroxycinnnamic acid in 60% acetonitrile/0.1% TFA) and directly spotted onto a MALDI target plate. Mass analyses were performed in a MALDI-TOF mass spectrometer (Voyager DE-STR, Applied Biosystems. Framingham, MA) equipped with a 337-nm nitrogen laser. Samples were analyzed in reflectron mode by TOF at an accelerating potential of 20 kV. The average of three scans (each containing 75 spectra) that passed the accepted criterion of peak intensity were automatically selected and saved using Data Explorer

software version 4.0 (Applied Biosystems). Mass spectra were automatically calibrated upon acquisition using two-point residual porcine trypsin autolytic fragments (842.51 and 2210.10 [M+H+] ions) and matrix-added standard bradykinin (Sigma) and ACTH (Sigma) peaks (757.39 and 2,465.19 [M+H+] ions). Raw spectra were baseline corrected and noise filtered (correlation factor = 7). Spectra were deisotoped, and the peaks were collected automatically using the "copy peak list" feature of the software. Extra peaks resulting from keratin and trypsin were removed manually from monoisotopic standard peak lists. All of the submitted masses were accurate to the level of 40 ppm.

2.9 Identification of proteins

Monoisotopic masses of each spectrum in triplicate were searched in the NCBI non-redundant database (NCBI nr 2005.01.03) using the ProFound-peptide mapping search engine (The Rockefeller University Edition, Version 2005.02.14). Identified proteins were confirmed via the MS-Fit search engine using SwissProt.07.05.2006 database. The SwissProt database was searched with restrictions by experimental molecular weight (20000–100000 Da), isoelectric point (p*I* 3.00–10.00), and species (*Rattus Norvegicus*) against 49,282 entries. Unmatched peptides and miscleavage sites were disregarded. All mass searches were performed with the short form of the Pro-Found-peptide mapping search engine in the *Rattus* taxonomic category for only single proteins with a pre-assumed experimental mass and p*I* range and crosschecked with the MS-Fit search engine. The search parameters were allowed complete modification with iodoacetamide. Peptides were matched with the theoretical peptide masses of all proteins from *Rattus Norvegicus* of the NCBI and SwissProt databases using a tolerance limit of 50 ppm. Other criteria for positive identification of proteins were set as follows: (1) the number of peptides matched averaged more than 10 (minimum, 5); (2) 20–50 ppm or better mass accuracy; (3) the matched peptides covered at least 15% of the whole protein sequence with a significant Z score (>90% probability) and higher Mowse score; (4) each identified protein was cross referenced to the comparable p*I* and molecular weight (kDa) obtained from experimental image analysis on the 2-DE gel. Among five maximum reported hits from the SwissProt database, the highest Mowse score (at least 25% coverage) with unique peptide and validation through Western blot analysis was used to eliminate the redundancy of the matched protein to multiple members of a protein family. A complete description of protein identification by peptide fingerprinting is given in the Supplementary Material (SM.1).

2. 10 Western blot analysis

The same protein samples that were used for 2-DE described above were also used for Western blotting analysis. The samples were heated for 5 min at 95°C and then loaded onto 4% stacking/10% separating SDS-polyacrylamide gels (20 μg protein/lane). The proteins were eletrophoretically transferred onto nitrocellulose membrane. The blotting membranes were blocked with 5% non-fat dry milk for 1 h and incubated overnight at 4°C with goat anti-glutamine synthetase (GS; 1:200; Santa Cruz Biotechnology, Inc., Santa Cruz, CA), goat anti-sarcomeric mitochondrial creatine kinase (S-MtCK; 1:200; Santa Cruz Biotechnology, Inc.), rabbit anti-guanine nucleotide-binding protein G (Go), alpha subunit 1 (1:1000; Calbiochem, San Diego, CA), rabbit anti-heat shock protein 84 (HSP84; 1:1000; Abcam Inc., Cambridge, MA), rabbit anti-heat shock cognate 70 (HSC70; 1:1000; StressGen Biotechnologies, Victoria, BC), rabbit anti-secreted frizzled-related protein 4 precursor (sFRP-4; 1:1000; prepared by A.M.D.), mouse anti-*N*-cadherin (1:1000; BD Transduction Laboratories, San Jose, CA), mouse anti-PSD-95 (1:1000; BD Transduction Laboratories), rabbit anti-synaptophysin (1:1000; BD Transduction Laboratories), or mouse anti-glyceraldehyde dehydrogenase (GAPDH; 1:1000; Santa Cruz Biotechnology, Inc.). *N*-cadherin and GAPDH were used as the loading controls for the synaptosomal membrane fraction [20] and total soluble fraction, respectively. The proteins were detected using anti-rabbit, anti-goat, or anti-mouse secondary antibody and visualized with chemiluminescence reagents provided with the ECL kit

(Amersham Pharmacia Biotech, Piscataway, NJ) and exposure to film. The fluorographic images were digitalized into eight-bit tagged image format files using scan jet Plus (Hawlett-Packard). Baseline density of the area surrounding the bands was determined by two-dimensional integration with quantity one image analysis software (Bio-Rad), and then local background was subtracted. The percent volume ratio of selected bands, i.e. total signal intensity inside a defined boundary drawn on an image, was used for densitometric analysis.

2. 11 Statistical Analysis

For behavioral testing, the pattern of positive and negative paw withdrawal responses to the von Frey filament stimulation was converted to a 50% threshold value using the formula provided by Dixon [14]. A two-way repeated measure ANOVA with Fisher's protected LSD post-hoc test was used to compare PWT difference between pre- and post-surgery conditions.

For Western blot analysis, the relative density of each protein was calculated by dividing the optical density value of each protein by the optical density of the corresponding loading control (*N*-cadherin for the synaptosomal fraction and GAPDH for the total soluble fraction). An independent Student's *t* test was used to compare the relative density differences between the SNI and sham groups. Data are presented as mean ± standard error of mean (S.E.M). $P < 0.05$ was considered statistically significant in all tests. The statistical software package SigmaStat (Systat, Port Richard, CA) was used to perform all statistical analyses.

3 Results and discussion

3. 1 Induction of SNI-induced mechanical hypersensitivity in rats

To ensure that all SNI rats used in the proteomic study showed pain hypersensitivity, rat PWTs in response to mechanical stimuli were measured. Consistent with our previously published data [11,21,22], SNI induced mechanical hypersensitivity, as indicated by a significant decrease in PWT on the ipsilateral side (but not on the contralateral side) on day 14 post-surgery compared to the baseline (Fig. 1A, n = 9; $P < 0.01$). Sham surgery did not cause mechanical hypersensitivity on either the ipsilateral or contralateral side (Fig. 1B, n = 9, $P > 0.05$).

3.2 Identification of differentially expressed proteins in ipsilateral dorsal horn following SNI

To investigate the synaptic basis of SNI-induced mechanical hypersensitivity at the spinal cord level, we first collected the crude synaptosomal membrane fraction by velocity gradient centrifugation [15,16]. To test the specificity of the fractionation procedure, the expression levels of a plasma membrane–specific protein, *N*-cadherin, a synaptic vesicle membrane protein, synaptophysin, a postsynaptic density protein, PSD-95, and GAPDH, an intracellular protein, were assessed in both crude synaptosomal membrane and cytosolic fractions. Consistent with previous studies [15,16,20], N-cadherin, PSD-95, and synaptophysin were expressed highly in the crude synaptosomal fraction but weakly or undetectablely in the cytosolic fractions (Fig. 2). In contrast, GAPDH was expressed predominantly in the crude cytosolic fraction but weakly in the synaptosomal membrane fraction (Fig. 2). These data indicate that the fractionation procedure used effectively separates synaptosome-associated proteins from cytosolic proteins.

We then compared the expression of synaptosome-associated proteins derived from ipsilateral dorsal horns of SNI- and sham-treated rats on day 14 post-surgery. More than 1500 proteins were captured in the pH range 5.0–9.5 (Fig. 3). Overall, the 2-DE protein spot patterns across all the gels from SNI-treated and sham groups were similar (Fig. 3A). In total, 30 protein spots (designated as SNI 1–30) that showed at least 2-fold difference in the spot relative volume between the Sham and SNI-treated groups were selected for protein identification and 27 of those were successfully characterized (Table 1). Of the 27 proteins, two, neurofilament triplet

L protein (SNI-5 in Figs. 3B and 4) and ATP synthase β chain (SNI-8 in Figs. 3B and 4), were down-regulated, and the remaining 25 were up-regulated (Figs. 3B and 4, Table 1). These 27 proteins are involved in transmission and modulation of nociceptive information, cellular metabolism, plasma membrane receptor trafficking, oxidative stress, apoptosis, and cell death (Table 1).

In previous proteomic studies [9,10], five proteins were shown to have significant differences in dorsal horn expression between the sham group and either SNI-treated or chronic constriction injury-treated groups. The major classes of these proteins related to oxidative stress, apoptosis, and cellular metabolism [9,10]. The reason for the discrepancy between the previous and present studies is unclear but may be related to the difference in sample preparation. In the previous studies, some synaptic membrane proteins might have been lost because the tissue supernatants were collected after very high speed centrifugation [9,10].

It should be noted that some proteins known to undergo expression changes in the spinal dorsal horn after peripheral nerve injury were not identified in either the previous [9,10] or current 2-DE–based study. For example, peripheral nerve injury significantly increases protein expression of synaptic AMPA receptor subunits GluR1 and GluR2, protein kinase C alpha, protein kinase C beta 1, and calcium channel alpha 2/delta subunit 1 in dorsal horn [3,23-25]. These changes might not have been detected by proteomic analysis because of the limitation of the 2-DE proteomic approach. Our 2-DE gels displayed approximately 1500 distinct protein spots, which cover only a fraction of the total population of dorsal horn proteins. Many synaptic proteins (e.g., transmembrane receptors and ion channels) have physical properties, such as high molecular weight, extreme p*I*, and/or a high degree of overall hydrophobicity, that prohibit their resolution on a 2-DE gel [26]. In addition, the synaptosomal fraction that we collected is crude because differential centrifugation cannot completely separate synaptosome from intracellular organic membranes (Table 1). Furthermore, the expression changes of proteins that are at very low quantities in crude synaptosomal fraction might not be detected by 2-DE gels. Therefore, more in-depth proteomics analysis that focuses on the postsynaptic density proteome, for example, may be expected to cover larger categories of protein groups [26].

To confirm the reliability of our proteomic analysis, we randomly selected six proteins for Western blot analysis. As shown in Fig. 5, the up-regulation of GS, S-MtCK, Go alpha subunit 1, HSP84, HSC70, and sFRP-4 was validated in the dorsal horn synaptosomal fraction. Interestingly, we found that, in the dorsal horn total soluble fraction, of the six proteins, only GS expression was significantly increased (Fig. 6). These results indicate that peripheral nerve injury insult might lead not only to changes in protein expression but also to changes in subcellular distribution of proteins in dorsal horn cells.

SNI-induced changes of protein expression in dorsal horn are thought to be part of the central mechanism underlying neuropathic pain [2]. Recently, trafficking of postsynaptic membrane proteins (e.g. AMPA receptors) has been recognized as a central mechanism in various forms of synaptic plasticity [27,28]. Thus, SNI-induced changes in both expression and subcellular distribution of dorsal horn proteins might participate in the maintenance of peripheral nerve injury–induced pain hypersensitivity. However, the change in dorsal horn protein subcellular distribution might need to be further confirmed by specific approaches of protein trafficking (e.g., surface biotinylation assay and electron microscopy) [21] because our present data can not rule out the possibility that expression changes in the total soluble fraction are undetectable by Western blot analysis when the proteins are present only at very low levels.

3.3 SNI-induced up-regulation of proteins involved in transmission and modulation of noxious information in dorsal horn

An important observation in the present 2-DE–based study is that SNI increased the expression of the synaptosome-associated proteins that are involved in transmission and modulation of noxious information in the dorsal horn (Table 1). Of these proteins, GS (SNI-17 in Figs. 3B and 4, Table 1) and glutamate dehydrogenase 1 (SNI-15 in Figs. 3B and 4, Table 1) are key enzymes that are involved in regulation of glutamate metabolism and excitatory synaptic transmission in the central nervous system [29]. Glutamate receptor activation plays a critical role in the spinal central mechanism that underlies the development and maintenance of neuropathic pain [2]. Intrathecal superfusion of a GS inhibitor significantly attenuates the central sensitization of nociceptive neurons in rat medullary dorsal horn after peripheral inflammation [29]. Thus, SNI-induced up-regulation of dorsal horn GS and glutamate dehydrogenase 1 might participate in the central sensitization that underlies neuropathic pain.

Our 2-DE gels displayed an increase of 5-hydroxytryptamine (5-HT) 2A receptor in dorsal horn synaptosome on day 14 post-SNI (SNI-14 in Figs. 3B and 4). 5-HT modulates the transmission of nociceptive information in dorsal horn [2]. Also, the activation of spinal 5-HT-2A/2C receptors increases the pain-like behavioral responses in both the early and late phases of the formalin model [30]. 5-HT-2A receptor knockout mice display a dramatic decrease in the formalin-induced nociceptive responses for the late phase [31]. It appears that SNI-induced up-regulation of 5-HT-2A receptor in dorsal horn synaptosome might be involved in the maintenance of pain hypersensitivity underlying neuropathic pain.

We also observed increased levels of neuronal acetylcholine (Ach) receptor alpha 2 subunit (SNI-7 in Figs. 3B and 4, Table 1) and GABAA receptor rho-2 subunit (SNI-12 in Figs. 3B and 4, Table 1) in dorsal horn synaptosome on day 14 post-SNI. Consistent with our finding, a previous study reported that the muscarinic Ach receptor was up-regulated in the dorsal spinal cord in a model of neuropathic pain [32]. Spinal activation of both Ach receptors and GABAA receptors produced antinocicpetion in neuropathic pain [32,33]. The significance of the increase in these two inhibitory receptors in neuropathic pain is unknown, but the increase of Ach receptor alpha 2 subunit expression probably accounts for the increased efficacy of its antinociceptive effects in neuropathic pain; intrathecal injection of a small dose of an Ach receptor agonist produces a profound anti-allodynic effect in rats with neuropathy [34].

3.4 SNI-induced changes in the expression of proteins involved in increased cellular metabolism in dorsal horn

Cellular metabolic activities in dorsal horn are increased under neuropathic pain conditions. Using the [^{14}C]-2-deoxyglucose technique, previous investigators showed that peripheral nerve injury produced a significant increase in glucose utilization in dorsal horn [35,36]. In addition, lipid metabolism is intensified following peripheral noxious stimulation [37]. Our 2-DE–based study consistently demonstrated that SNI altered expression of cellular metabolism–associated proteins in dorsal horn (Table 1). Three such proteins up-regulated in the dorsal horn synaptosomal fraction on day 14 post-SNI were pyruvate kinase isozymes M1/M2 and gamma-enoclase (SNI-9 and 11 in Figs. 3B and 4), which participate in glycolysis [38,39], and 2,4-dienoyl-CoA reductase (SNI-25 in Figs.3B and 4,Table 1), which is involved in the metabolism of unsaturated fatty acid [40]. We also found that S-MtCK protein, which plays a central role in mitochondrial energy transduction [41], and transcription factor A, which is involved in mitochondrial transcription regulation [42], were increased more than 3-fold after SNI (SNI-19 and 20 in Figs. 3B and 4). In addition, ATP synthase alpha chain (SNI-16 in Figs 3B and 4) was up-regulated, although ATP synthase beta chain (SNI-8 in Figs 3B and 4) was down-regulated after SNI. Taken together, these data provide additional evidence that cellular metabolic activities, especially those involved in energy metabolism, are increased in dorsal

horn under neuropathic pain conditions. This increase might be necessary to meet the increasing energy demands for nerve injury-evoked hyperactivity of neurons and glia in dorsal horn.

3.5 SNI-induced increases in proteins involved in dorsal horn plasma membrane receptor trafficking

Plasma membrane receptors (e.g., AMPA receptors) are constitutively trafficked between the synaptic membrane and the intracellular compartment via vesicle-mediated membrane fusion (exocytosis) and endocytosis [27,28]. Regulation of membrane fusion or endocytosis might result in a rapid change in the number of receptors expressed on the synaptic membrane and in receptor-mediated responses. Five proteins identified to be up-regulated in our 2-DE–based study (Figs. 3B and 4) might play a critical role in regulating membrane receptor trafficking. The first, SH3-containing GRB2-like protein 1, which interacts selectively with synaptojanin and dynamin I, is involved in synaptic vesicle recycling [43]. Another cellular growth-associated protein, septin-5, has a role in membrane fusion during exocytosis by interacting with syntaxin and synaptophysin [44]. The alpha isoform of phosphatidylinositol transfer protein, which is responsible for the transport of phosphatidylinositol, was found to be involved in vesicle transport and in cytoskeletal function [45]. Transitional endoplasmic reticulum ATPase, a ubiquitous clathrin-binding protein, and beta-adducin, a membrane cytoskeleton-associated protein, are required for clathrin-coated vesicle-mediated endocytosis [46-48]. Thus, SNI-induced increases in these five proteins may regulate the receptor trafficking in dorsal horn during the maintenance phase of neuropathic pain. A previous study reported that capsaicin-induced visceral noxious insult rapidly increased the level of AMPA receptor subunit GluR1 protein in the spinal cord membrane fraction, with a corresponding decrease in the amount of GluR1 in the cytosolic fraction [20]. Whether peripheral nerve injury alters the trafficking of plasma membrane receptors (such as AMPA receptors) and whether these proteins participate in nerve injury-induced receptor trafficking in dorsal horn neurons remain to be explored.

3.6 SNI-induced alteration of proteins involved in oxidative stress, apoptosis, and degeneration in dorsal horn

Peripheral nerve injury could cause oxidative stress, apoptosis, and cell death in dorsal horn cells [49,50]. However, the underlying molecular mechanisms are still elusive. HSP84 promotes the degradation of oxidized proteins under conditions of oxidative stress [51]. sFRP4 antagonizes a molecular pathway for cell survival and is associated with apoptosis [52]. The Go alpha subunit 1 is involved in amyloid beta-induced neuronal degeneration in Alzheimer's disease [53,54]. Our study showed that the expression levels of these three proteins were increased in the dorsal horn synaptosomal fraction (Figs. 3B,4) without significant changes in total soluble fraction on day 14 post-SNI (Fig. 6). These results suggest that SNI-induced translocation of these proteins into the synaptosomal fraction might be involved in oxidative stress, apoptosis, and cell death under neuropathic pain conditions [49,50].

Interestingly, HSC70, which protects against oxidative damage [55], was also found to be translocated into the synaptosomal fraction on day 14 post-SNI (Figs 3B,4,5, and 6). The expression of two other protective proteins, cysteine dioxygenase type 1, which protects against cytotoxicity [56], and beta-hexosaminidase alpha chain precursor, the absence of which causes GM2 ganglioside accumulation and neurodegeneration [57], was increased in dorsal horn synaptosome in our 2-DE gels (SNI-13 and SNI-28 in Figs. 3B and 4). SNI-induced changes in translocation or expression of these three proteins might protect the cells from SNI-induced excitotoxicity in dorsal horn under neuropathic pain conditions. Among small heat-shock proteins, heat-shock protein beta-8 (HSP22) has either pro-or anti-apoptotic effects [58]; its expression was increased by approximately 4.5-fold in dorsal horn on day 14 post-SNI (SNI-29

in Figs 3B and 4). The function of this protein in neuropathic pain is unclear and remains to be defined.

Neurofilaments are the putative biological markers of axonal and neuronal degeneration [59]. The expression level of neurofilament triplet L protein, one of the type-IV neurofilament proteins, was reduced in dorsal horn after SNI in our 2-DE–based study (SNI-5 in Figs. 3B and 4). Peripheral inflammation also led to its reduction in spinal dorsal horn [10,60], indicating that neurofilament triplet L protein might be involved in dorsal horn neuronal degeneration under neuropathic and inflammatory pain conditions. Interestingly, alpha-internexin, another type-IV filament protein, was over-expressed by approximately 2-fold in dorsal horn synaptosomal fraction on day 14 post-SNI (SNI-6 in Figs. 3B and 4). The significance of this increase is unknown, but the results suggest that the functions of these two type-IV filament proteins differ in neuropathic pain.

2′,3′-cyclic-nucleotide 3′-phosphodiesterase (CNPase) is found almost exclusively in the oligodendrocytes of the central nervous system. Mice lacking expression of CNPase have disrupted axoglial interactions that might underlie progressive axonal degeneration [61]. Our 2-DE gels showed a more than 6-fold up-regulation of CNPase in the dorsal horn synaptosomal fraction on day 14 post-SNI (SNI-18 in Figs. 3B and 4). Although the significance of this increase is unclear, this protein might be involved in axonal regeneration via promotion of axon-glia interactions under neuropathic pain conditions.

4 Concluding remarks

In summary, our analysis provides an overview of proteomic changes in the dorsal horn synaptosome during the maintenance phase of neuropathic pain. This study demonstrates that peripheral nerve injury alters the expression and/or subcellular distribution of some specific dorsal horn proteins that are involved in transmission and modulation of noxious information, cellular metabolism, plasma membrane receptor trafficking, oxidative stress, apoptosis, and degeneration under neuropathic pain conditions. Our 2-DE gel profiles were highly reproducible, an essential trait for further development of a neuropathic pain database. In addition, the majority of the proteomic changes were consistent with the current proposed mechanisms of neuropathic pain. These changes might participate in the central mechanism that underlies the maintenance of neuropathic pain.

Supplementary Material

Refer to Web version on PubMed Central for supplementary material.

Acknowledgments

This work was supported by National Institutes of Health Grants NS 058886 and NS 057343 and the Johns Hopkins University Blaustein Pain Research Fund (to Y.-X. T). The authors thank Claire Levine, MS, for her editorial assistance.

Abbreviations

2-DE
two-dimensional electrophoresis

5-HT
5-hydroxytryptamine

Ach
acetylcholine

HSP84
heat shock protein 84

HSC70
heat shock cognate 70

GAPDH
glyceraldehyde dehydrogenase

Go
nucleotide-binding protein G

GS
glutamine synthetase

IEF
isoelectric focusing

IPG
immobilized pH gradient

PWTs
paw withdrawal thresholds

sFRP-4
secreted frizzled-related protein 4 precursor

S-MtCK
sarcomeric mitochondrial creatine kinase

SNI
spinal nerve injury

References

1. Campbell JN, Meyer RA. Mechanisms of neuropathic pain. Neuron 2006;52:77–92. [PubMed: 17015228]
2. Woolf, CJ.; Salter, MW. Wall and Melzack's Textbook of Pain. McMahon, S.; Koltzenburg, M., editors. Elsevier; London: 2006. p. 91-105.
3. Yang L, Zhang FX, Huang F, Lu YJ, et al. Peripheral nerve injury induces trans-synaptic modification of channels, receptors and signal pathways in rat dorsal spinal cord. Eur J Neurosci 2004;19:871–883. [PubMed: 15009134]
4. Coyle DE. Spinal cord transcriptional profile analysis reveals protein trafficking and RNA processing as prominent processes regulated by tactile allodynia. Neuroscience 2007;144:144–56. [PubMed: 17069981]
5. Rodriguez PJ, Korostynski M, Kaminska-Chowaniec D, Obara I, et al. Comparison of gene expression profiles in neuropathic and inflammatory pain. J Physiol Pharmacol 2006;57:401–14. [PubMed: 17033093]
6. Ji RR, Samad TA, Jin SX, Schmoll R, et al. p38 MAPK activation by NGF in primary sensory neurons after inflammation increases TRPV1 levels and maintains heat hyperalgesia. Neuron 2002;36:57–68. [PubMed: 12367506]
7. Becker M, Schindler J, Nothwang HG. Neuroproteomics - the tasks lying ahead. Electrophoresis 2006;27:2819–29. [PubMed: 16739225]
8. Marcus K, Schmidt O, Schaefer H, Hamacher M, et al. Proteomics--application to the brain. Int Rev Neurobiol 2004;61:285–311. [PubMed: 15482819]
9. Lee SC, Yoon TG, Yoo YI, Bang YJ, et al. Analysis of spinal cord proteome in the rats with mechanical allodynia after the spinal nerve injury. Biotechnol Lett 2003;25:2071–8. [PubMed: 14969411]

10. Kunz S, Tegeder I, Coste O, Marian C, Pfenninger A, Corvey C, Karas M, Geisslinger G, Niederberger E. Comparative proteomic analysis of the rat spinal cord in inflammatory and neuropathic pain models. Neurosci Lett 2005;81:289–93. [PubMed: 15896486]
11. Zhang B, Tao F, Liaw WJ, Bredt DS, et al. Effect of knock down of spinal cord PSD-93/chapsin-110 on persistent pain induced by complete Freund's adjuvant and peripheral nerve injury. Pain 2003;106:187–96. [PubMed: 14581127]
12. Kim SH, Chung JM. An experimental model for peripheral neuropathy produced by segmental spinal nerve ligation in the rat. Pain 1992;50:355–63. [PubMed: 1333581]
13. Chaplan SR, Bach FW, Pogrel JW, Chung JM, et al. Quantitative assessment of tactile allodynia in the rat paw. J Neurosci Methods 1994;53:55–63. [PubMed: 7990513]
14. Dixon WJ. Efficient analysis of experimental observations. Annu Rev Pharmacol Toxicol 1980;20:441–62. [PubMed: 7387124]
15. Dunah AW, Standaert DG. Dopamine D1 receptor-dependent trafficking of striatal NMDA glutamate receptors to the postsynaptic membrane. J Neurosci 2001;21:5546–58. [PubMed: 11466426]
16. Lee SH, Valtschanoff JG, Kharazia VN, Weinberg R, et al. Biochemical and morphological characterization of an intracellular membrane compartment containing AMPA receptors. Neuropharmacology 2001;41:680–92. [PubMed: 11640922]
17. Singh OV, Vij N, Mogayzel PJ Jr, Jozwik C, et al. Pharmacoproteomics of 4-phenylbutyrate-treated IB3-1 cystic fibrosis bronchial epithelial cells. J Proteome Res 2006;5:562–71. [PubMed: 16512671]
18. Singh OV, Pollard HB, Zeitlin PL. Chemical rescue of ΔF508-CFTR mimics genetic repair in cystic fibrosis bronchial epithelial cells. Molecular & Cellular Proteomics 2008;7:1099–110. [PubMed: 18285607]
19. Wheelock AM, Buckpitt AR. Software-induced variance in two-dimensional gel electrophoresis image analysis. Electrophoresis 2005;26:4508–20. [PubMed: 16315176]
20. Galan A, Laird JM, Cervero F. In vivo recruitment by painful stimuli of AMPA receptor subunits to the plasma membrane of spinal cord neurons. Pain 2004;112:315–23. [PubMed: 15561387]
21. Tao YX, Rumbaugh G, Wang GD, Petralia RS, et al. Impaired NMDA receptor-mediated postsynaptic function and blunted NMDA receptor-dependent persistent pain in mice lacking postsynaptic density-93 protein. J Neurosci 2003;23:6703–12. [PubMed: 12890763]
22. Guan Y, Yaster M, Raja SN, Tao YX. Genetic knockout and pharmacologic inhibition of neuronal nitric oxide synthase attenuate nerve injury-induced mechanical hypersensitivity in mice. Mol Pain 2007;3:29. [PubMed: 17922909]
23. Garry EM, Moss A, Rosie R, Delaney A, et al. Fleetwood-Walker SM. Specific involvement in neuropathic pain of AMPA receptors and adapter proteins for the GluR2 subunit. Mol Cell Neurosci 2003;24:10–22. [PubMed: 14550765]
24. Harris JA, Corsi M, Quartaroli M, Arban R, et al. Upregulation of spinal glutamate receptors in chronic pain. Neuroscience 1996;74:7–12. [PubMed: 8843072]
25. Lim J, Lim G, Sung B, Wang S, et al. Intrathecal midazolam regulates spinal AMPA receptor expression and function after nerve injury in rats. Brain Res 2006;1123:80–88. [PubMed: 17049496]
26. Li KW, Hornshaw MP, Van Der Schors RC, Watson R, et al. Proteomics analysis of rat brain postsynaptic density. Implications of the diverse protein functional groups for the integration of synaptic physiology. J Biol Chem 2004;279:987–1002. [PubMed: 14532281]
27. Derkach VA, Oh MC, Guire ES, Soderling TR. Regulatory mechanisms of AMPA receptors in synaptic plasticity. Nat Rev Neurosci 2007;8:101–13. [PubMed: 17237803]
28. Greger IH, Esteban JA. AMPA receptor biogenesis and trafficking. Curr Opin Neurobiol 2007;17:289–97. [PubMed: 17475474]
29. Chiang CY, Wang J, Xie YF, Zhang S, et al. Astroglial glutamate-glutamine shuttle is involved in central sensitization of nociceptive neurons in rat medullary dorsal horn. J Neurosci 2007;27:9068–76. [PubMed: 17715343]
30. Kjørsvik A, Tjølsen A, Hole K. Activation of spinal serotonin(2A/2C) receptors augments nociceptive responses in the rat. Brain Res 2001;910:179–81. [PubMed: 11489268]
31. Kayser V, Elfassi IE, Aubel B, Melfort M, et al. Mechanical, thermal and formalin-induced nociception is differentially altered in 5-HT1A-/-, 5-HT1B-/-, 5-HT2A-/-, 5-HT3A-/- and 5-HTT-/- knock-out male mice. Pain 2007;130:235–48. [PubMed: 17250964]

32. Chen SR, Pan HL. Up-regulation of spinal muscarinic receptors and increased antinociceptive effect of intrathecal muscarine in diabetic rats. J Pharmacol Exp Ther 2003;307:676–81. [PubMed: 12966147]
33. Malan TP, Mata HP, Porreca F. Spinal GABA(A) and GABA(B) receptor pharmacology in a rat model of neuropathic pain. Anesthesiology 2002;96:1161–7. [PubMed: 11981157]
34. Chen SR, Khan GM, Pan HL. Antiallodynic effect of intrathecal neostigmine is mediated by spinal nitric oxide in a rat model of diabetic neuropathic pain. Anesthesiology 2001;95:1007–12. [PubMed: 11605898]
35. Price DD, Mao JR, Coghill RC, d'Avella D, et al. Regional changes in spinal cord glucose metabolism in a rat model of painful neuropathy. Brain Res 1991;64:314–8. [PubMed: 1810630]
36. Mao J, Price DD, Coghill RC, Mayer DJ, et al. Spatial patterns of spinal cord [14C]-2-deoxyglucose metabolic activity in a rat model of painful peripheral mononeuropathy. Pain 1992;50:89–100. [PubMed: 1325049]
37. Benani A, Vol C, Heurtaux T, Asensio C, Dauca M, et al. Up-regulation of fatty acid metabolizing-enzymes mRNA in rat spinal cord during persistent peripheral local inflammation. Eur J Neurosci 2003;18:1904–14. [PubMed: 14622223]
38. Muñoz ME, Ponce E. Pyruvate kinase: current status of regulatory and functional properties. Comp Biochem Physiol B Biochem Mol Biol 2003;135:197–218. [PubMed: 12798932]
39. Nucci P, Tredici G, Manitto MP, Alfarano R, et al. Neuron-specific enolase in ophthalmology. Arch Ital Anat Embriol 1991;96:73–6. [PubMed: 1781726]
40. Clejan S, Schulz H. Effect of growth hormone on fatty acid oxidation: growth hormone increases the activity of 2,4-dienoyl-CoA reductase in mitochondria. Arch Biochem Biophys 1986;246:820–8. [PubMed: 3707134]
41. Payne RM, Strauss AW. Expression of the mitochondrial creatine kinase genes. Mol Cell Biochem 1994;133-134:235–43. [PubMed: 7808456]
42. Clayton DA. Transcription and replication of animal mitochondrial DNAs. Int Rev Cytol 1992;141:217–32. [PubMed: 1452432]
43. Ringstad N, Nemoto Y, De Camilli P. The SH3p4/Sh3p8/SH3p13 protein family: Binding partners for synaptojanin and dynamin via a Grb2-like Src homology 3 domain. Proc Natl Acad Sci U S A 1997;94:8569–8574. [PubMed: 9238017]
44. Capurso G, Crnogorac-Jurcevic T, Milione M, Panzuto F, Campanini N, et al. Peanut-like 1 (septin 5) gene expression in normal and neoplastic human endocrine pancreas. Neuroendocrinology 2005;81:311–21. [PubMed: 16179808]
45. Liscovitch M, Cantley LC. Signal transduction and membrane traffic: the PITP/phosphoinositide connection. Cell 1995;81:659–62. [PubMed: 7774006]
46. Pleasure IT, Black MM, Keen JH. Valosin-containing protein, VCP, is a ubiquitous clathrin-binding protein. Nature 1993;365:459–62. [PubMed: 8413590]
47. Poupon V, Girard M, Legendre-Guillemin V, Thomas S, et al. Clathrin light chains function in mannose phosphate receptor trafficking via regulation of actin assembly. Proc Natl Acad Sci U S A 2008;105:168–73. [PubMed: 18165318]
48. Rabenstein RL, Addy NA, Caldarone BJ, Asaka Y, et al. Impaired synaptic plasticity and learning in mice lacking beta-adducin, an actin-regulating protein. J Neurosci 2005;25:2138–45. [PubMed: 15728854]
49. Whiteside GT, Munglani R. Cell death in the superficial dorsal horn in a model of neuropathic pain. J Neurosci Res 2001;64:168–73. [PubMed: 11288144]
50. Park ES, Gao X, Chung JM, Chung K. Levels of mitochondrial reactive oxygen species increase in rat neuropathic spinal dorsal horn neurons. Neurosci Lett 2006;391:108–11. [PubMed: 16183198]
51. Whittier JE, Xiong Y, Rechsteiner MC, Squier TC. Hsp90 enhances degradation of oxidized calmodulin by the 20 S proteasome. J Biol Chem 2004;279:46135–42. [PubMed: 15319444]
52. Drake JM, Friis RR, Dharmarajan AM. The role of sFRP4, a secreted frizzled-related protein, in ovulation. Apoptosis 2003;8:389–97. [PubMed: 12815282]
53. Tsukamoto E, Hashimoto Y, Kanekura K, Niikura T, et al. Characterization of the toxic mechanism triggered by Alzheimer's amyloid-beta peptides via p75 neurotrophin receptor in neuronal hybrid cells. J Neurosci Res 2003;73:627–36. [PubMed: 12929130]

54. Sola Vigo F, Kedikian G, Heredia L, Heredia F, et al. Amyloid-beta precursor protein mediates neuronal toxicity of amyloid beta through Go protein activation. Neurobiol Aging. 2008in print

55. Dastoor Z, Dreyer J. Nuclear translocation and aggregate formation of heat shock cognate protein 70 (Hsc70) in oxidative stress and apoptosis. J Cell Sci 2000;113:2845–54. [PubMed: 10910769]

56. Dominy JE Jr, Hwang J, Stipanuk MH. Overexpression of cysteine dioxygenase reduces intracellular cysteine and glutathione pools in HepG2/C3A cells. Am J Physiol Endocrinol Metab 2007;293:E62–9. [PubMed: 17327371]

57. Chavany C, Jendoubi M. Biology and potential strategies for the treatment of GM2 gangliosidoses. Mol Med Today 1998;4:158–65. [PubMed: 9572057]

58. Shemetov AA, Seit-Nebi AS, Gusev NB. Structure, properties, and functions of the human small heat-shock protein HSP22 (HspB8, H11, E2IG1): A critical review. J Neurosci Res 2008;86:264–9. [PubMed: 17722063]

59. Zaffaroni M. Biological indicators of the neurodegenerative phase of multiple sclerosis. Neurol Sci 2003;24:S279–82. [PubMed: 14652789]

60. Kunz S, Niederberger E, Ehnert C, Coste O, et al. The calpain inhibitor MDL 28170 prevents inflammation-induced neurofilament light chain breakdown in the spinal cord and reduces thermal hyperalgesia. Pain 2004;110:409–18. [PubMed: 15275793]

61. Rasband MN, Tayler J, Kaga Y, Yang Y, et al. CNP is required for maintenance of axon-glia interactions at nodes of Ranvier in the CNS. Glia 2005;50:86–90. [PubMed: 15657937]

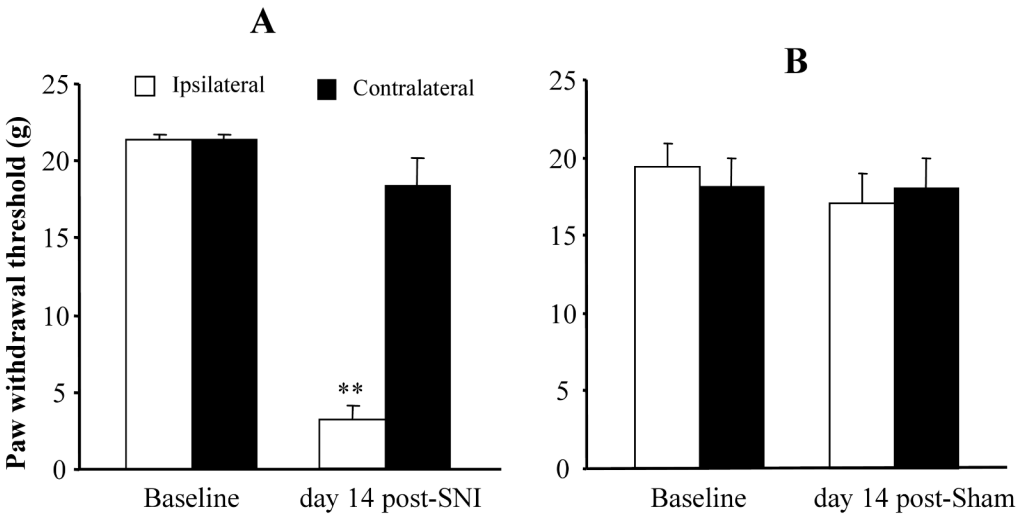

Figure 1.

Spinal nerve injury (SNI)-induced mechanical allodynia. (A) SNI led to a significant decrease in paw withdrawal threshold in response to mechanical stimuli on the ipsilateral, but not contralateral, side on day 14 after L5 SNI (n = 9); $^{**}P < 0.01$ *vs* the corresponding baseline. (B) Sham surgery did not produce a significant change in paw withdrawal threshold on either the ipsilateral or contralateral side on day 14 post-sham surgery (n = 9).

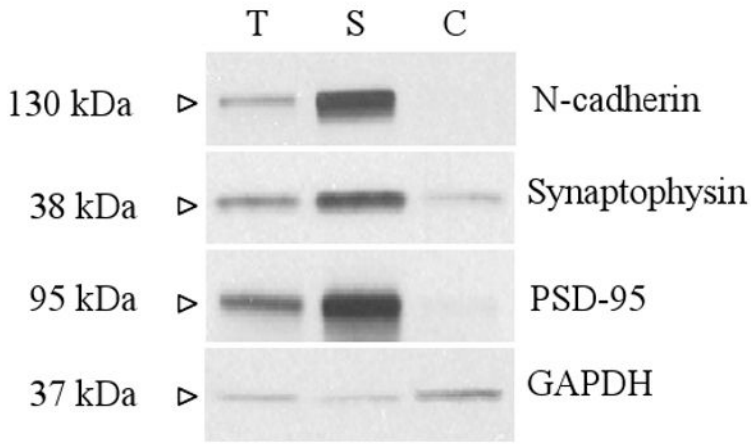

Figure 2.

The specificity of the fractionation procedure. The L5 dorsal horn tissues were collected, and three fractions, total soluble fraction (T), synaptosomal membrane fraction (S), and cytosolic fraction (C), were prepared as described in the Materials and Methods. The expression levels of *N*-cadherin (a plasma membrane–specific protein), synaptophysin (a synaptic vesicle membrane protein), PSD-95 (a postsynaptic density protein), and GAPDH (an intracellular protein) were examined in the total soluble fraction (T), synaptosomal membrane fraction (S), and cytosolic fraction (C).

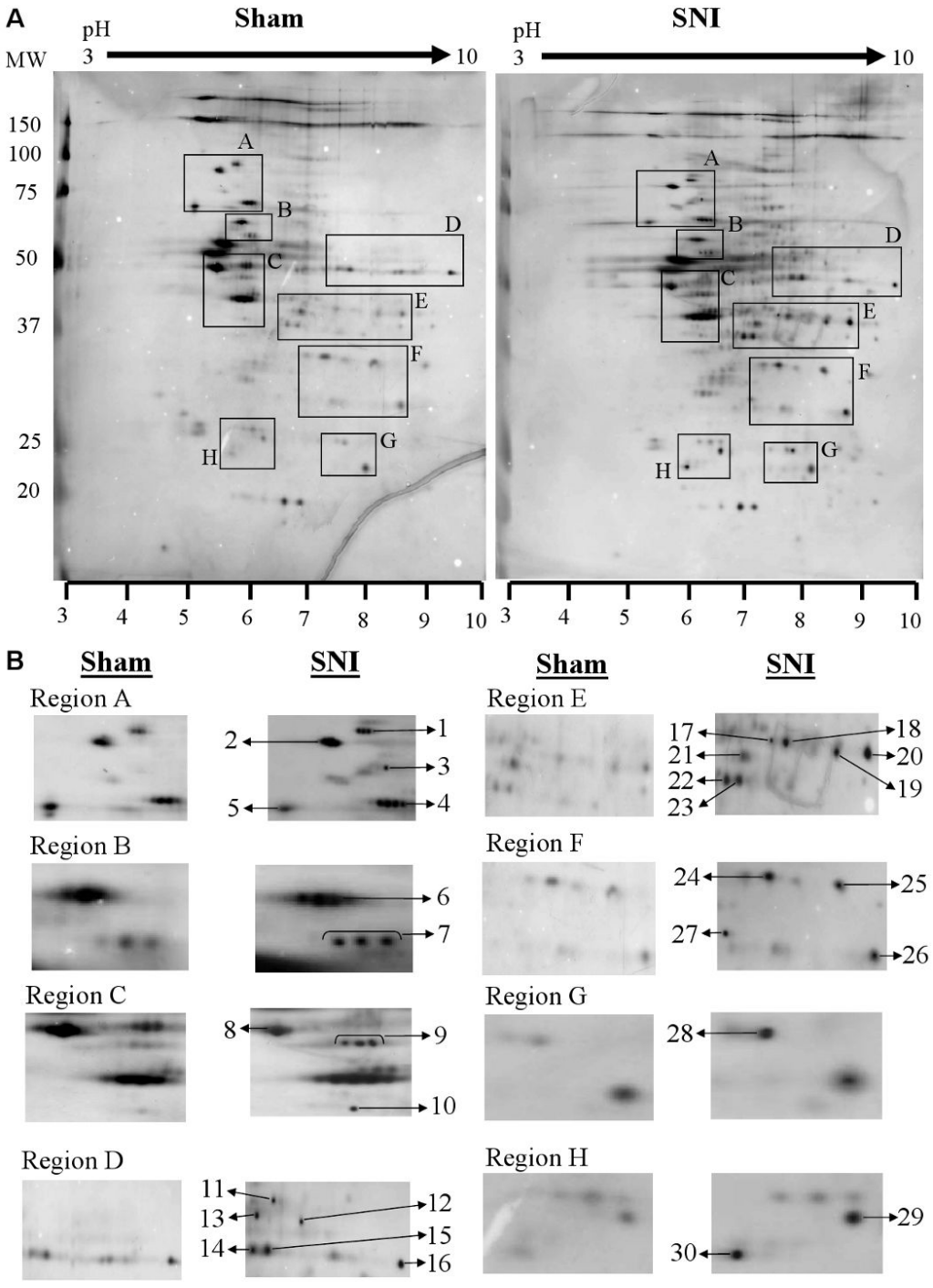

Figure 3.

Representative examples of silver-stained two-dimensional gels show expression maps of synaptosome-associated proteins in the ipsilateral dorsal horns of the fifth lumbar spinal cord segments derived from sham- and spinal nerve injury (SNI)-treated rats. Protein lysates were processed as described in the Materials and Methods. Protein samples (50 μg) were loaded onto IPG strips (pH 3–10 Non-Linear) and subsequently separated by mass on a 10% SDS-PAGE gel. The gel was stained with MS-compatible silver stain, and the filtered images were generated by Progenesis software (version 2005). (A) The outlined regions of interest

demarcate proteins that showed significant differences in expression between sham and SNI-treated groups. The patterns of protein spots on the two-dimensional gels were highly reproducible in six independent gels from three different experiments. (B) High magnification of the regions of interest from A. Significant protein spots that showed at least 2- fold difference in spot relative volume between Sham and SNI-treated groups were selected and labeled by arrows denoted as SNI-1 to SNI-30. The corresponding locations on the gels were excised, trypsinized, and analyzed by MALDI-TOF-MS as described in the Materials and Methods. The proteins were subsequently identified by tryptic peptide mass fingerprints. Table 1 contains a list of the identified proteins.

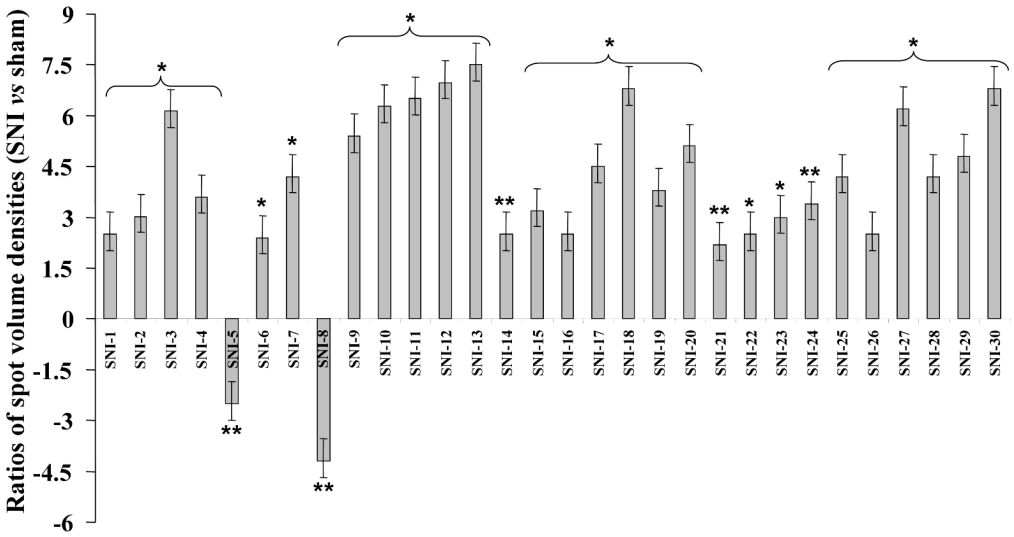

Figure 4.

Quantification of relative spot densities of identified and unidentified proteins. The Y-axis shows the ratios of spot volume densities, which were calculated by dividing the values of spot volume densities from the SNI-treated groups by the values of the corresponding spot volume densities from sham groups. The labels on the X-axis refer to the spots denoted as SNI-1 to SNI-30 in Figure 3B; n = 3 repeats (total 9 rats)/group. **P* < 0.05 and ***P* < 0.01 vs the sham group.

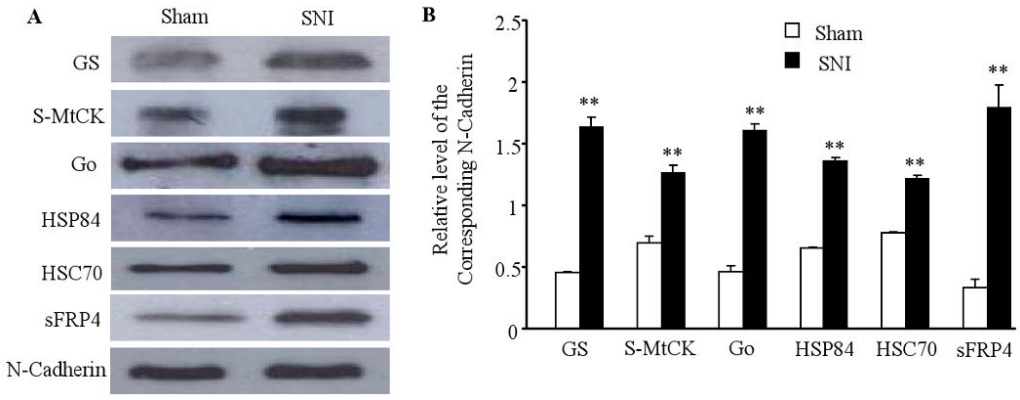

Figure 5.

Validation of SNI-induced expression changes of six randomly selected proteins identified by two-dimensional gel electrophoresis in dorsal horn synaptosomal fractions. (A) A representative example of Western blot analysis of glutamate synthetase (GS), sarcomeric mitochondrial creatine kinase (S-MtCK), guanine nucleotide-binding protein G (Go) alpha subunit 1, heat shock protein 84 (HSP84), heat shock cognate 70 (HSC70), and secreted frizzled-related protein 4 precursor (sFRP4) in sham and SNI-treated rats. (B) The statistical summary of the densitometric analysis expressed relative to the corresponding loading control (*N*-Cadherin). The data are presented as the mean ± SEM. n = 3 repeats (total 9 rats/group); $^{**}P < 0.01$ *vs* the corresponding sham group.

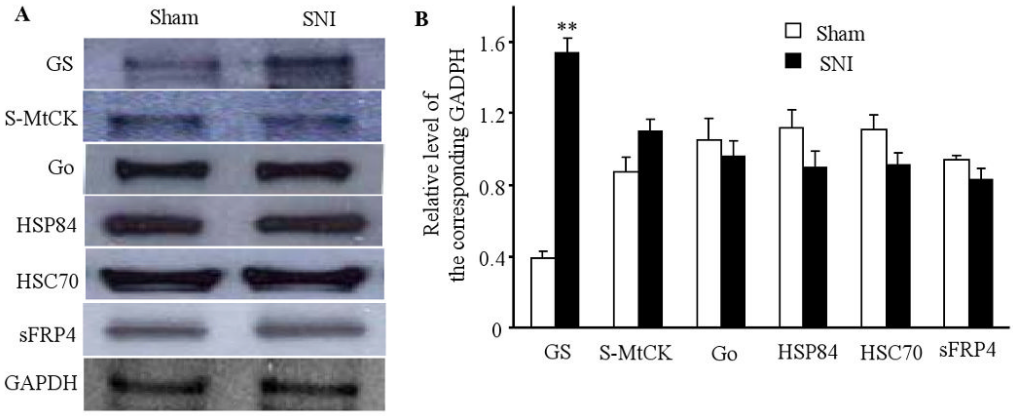

Figure 6.

Validation of SNI-induced expression changes of six randomly selected proteins identified by two-dimensional gel electrophoresis in dorsal horn total soluble fractions. (A) A representative example of Western blot analysis of GS, S-MtCK, Go, HSP84, HSC70, and sFRP4 in sham and SNI-treated rats. (B) The statistical summary of the densitometric analysis expressed relative to the corresponding loading control (glyceraldehyde dehydrogenase, GAPDH). The data are presented as the mean ± SEM. n = 3 repeats (9 rats/group); $^{**}P < 0.01$ *vs* the corresponding sham group.

Table 1

Differentially expressed protein spots with in-gel digestion and MALDI-TOF MS analysis. Spinal nerve injury-induced changes in expression of the proteins are indicated by up-arrows (increase) and down-arrows (decrease).

Spot No	Accession No	Protein name	Theoretical Mr (kDa)/p*I*	Observed Mr (kDa)/p*I*	Matching peptides (n)	Unmatched peptides (n)	Sequence coverage (%)	Expression
Proteins involved in transmission and modulation of noxious information								
SNI 7	P12389	Neuronal acetylcholine receptor protein, alpha-2 subunit precursor	58.61/5.2	57.8/5.1	15	21	25	↑
SNI 12	P47742	Gamma-aminobutyric-acid receptor rho-2 subunit precursor (GABA(A) receptor)	54.29/9.1	54.5/7.0	24	10	25	↑
SNI 14	P14842	5-hydroxytryptamine 2A receptor (5-HT-2A; Serotonin receptor 2A; 5-HT-2)	52.85/7.0	50.8/6.7	15	21	38	↑
SNI 15	P10860	Glutamate dehydrogenase 1, mitochondrialprecursor (GDH)	61.41/8.1	50.9/6.9	15	28	30	↑
SNI 17	P09606	Glutamine synthetase (Glutamate-ammonia ligase; GS)	42.26/6.6	41.8/6.7	8	26	22	↑
Proteins involved in cellular metabolism								
SNI 8	P10719	ATP synthase beta chain, mitochondrial precursor	56.35/5.2	51.2/4.9	15	17	45	↓
SNI 9	P07323	Gamma-enolase (2-phospho-D-glycerate hydro-lyase; Neural enolase; Neuron-specific enolase; NSE; Enolase 2)	47.14/5.0	58.4/5.1	27	5	56	↑
SNI 11	P11980	Pyruvate kinase isozymes M1/M2 (Pyruvate kinase muscle isozyme)	57.81/6.6	59.4/6.7	10	29	15	↑
SNI 16	P15999	ATP synthase alpha chain, mitochondrial precursor	59.75/9.2	51.3/9.1	12	38	28	↑
SNI 19	P09605	Creatine kinase, sarcomeric mitochondrial precursor (S-MtCK; Mib-CK; Basic-type mitochondrial creatine kinase)	47.38/8.8	43.7/7.1	23	18	26	↑
SNI 25	Q64591	2,4-dienoyl-CoA reductase, mitochondrial precursor [4-enoyl-CoA reductase (NADPH)]	42.85/6.3	36.5/7.7	7	21	24	↑
SNI 26	Q91ZW1	Transcription factor A, mitochondrial precursor (mtTFA)	28.18/9.8	29.5/7.5	9	25	37	↑
Proteins involved in plasma membrane receptor trafficking								
SNI 1	P46462	Transitional endoplasmic reticulum ATPase (TER ATPase; 15S Mg(2+)-ATPase p97 Subunit; Valosin-containing protein; VCP)	89.35/5.1	88.5/5.2	62	15	47	↑
SNI 3	Q05764	Beta-adducin (Erythrocyte adducin beta Subunit; Adducin 63)	80.59/5.7	82.7/5.6	60	37	41	↑
SNI 22	O35964	SH3-containing GRB2-like protein 1 (SH3domain protein 2B; SH3p8)	41.49/5.4	41.5/5.6	40	15	52	↑
SNI 23	Q9JJM9	Septin-5 (Peanut-like protein 1; Cell division control-related protein 1)	42.85/6.3	41.8/5.8	30	23	44	↑
SNI 27	P16446	Phosphatidylinositol transfer protein alpha isoform (PtdIns transfer protein alpha; PtdInsTP; PI-TP-alpha)	31.90/6.0	30.5/6.0	28	31	69	↑
Proteins involved in oxidative stress, apoptosis, and degeneration								

Spot No	Accession No	Protein name	Theoretical Mr (kDa)/p*I*	Observed Mr (kDa)/p*I*	Matching peptides (n)	Unmatched peptides (n)	Sequence coverage (%)	Expression
SNI 2	P34058	Heat shock protein HSP 90-beta (HSP 84)	83.31/5.1	83.5/5.0	24	18	29	↑
SNI 4	P63017	Heat shock cognate 71 kDa protein (Heat shock 70 kDa protein 8)	70.8/5.4	70.5/5.3	24	20	36	↑
SNI 5	P19527	Neurofilament triplet L protein (68 kDa neurofilament protein; Neurofilament light polypeptide; NF-L)	61.33/4.6	60.6/4.7	16	26	20	↓
SNI 6	P23565	Alpha-internexin (Alpha-Inx)	56.11/5.2	57.5/5.1	13	32	37	↑
SNI 10	P59215	Guanine nucleotide-binding protein Go, alpha subunit 1	40.06/5.3	39.7/5.2	9	18	29	↑
SNI 13	Q641X3	Beta-hexosaminidase alpha chain precursor (N-acetyl-beta-glucosaminidase; Beta-N-Acetylhexosaminidase; Hexosaminidase A)	60.53/6.8	59.7/6.7	6	24	12	↑
SNI 18	P13233	2′,3′-cyclic-nucleotide 3′-phosphodiesterase (CNP; CNPase)	47.26/9.0	42.6/6.8	11	18	26	↑
SNI 20	Q9JLS4	Secreted frizzled-related protein 4 precursor (sFRP-4)	39.76/9.0	40.5/7.5	19	25	31	↑
SNI 28	P21816	Cysteine dioxygenase type 1 (Cysteine dioxygenase type I; CDO; CDO-I)	23.02/6.0	24.6/6.0	5	11	20	↑
SNI 29	Q9EPX0	Heat-shock protein beta-8 (HspB8; Alpha crystallin C chain; Small stress protein-like protein HSP22)	21.59/4.9	23.5/4.7	15	14	30	↑
		Unidentified (UI) proteins						
SNI 21	UI	UI	UI	44.5/6.2	UI	66	UI	↑
SNI 24	UI	UI	UI	55.2/6.8	UI	38	UI	↑
SNI 30	UI	UI	UI	22.5/4.5	UI	45	UI	↑